

Near-infrared coronagraph imager on the Subaru 8m telescope

Koji Murakawa¹, Hiroshi Suto¹, Motohide Tamura², Hideki Takami¹, Naruhisa Takato¹,
Saeko S. Hayashi¹, Yoshiyuki Doi¹, Norio Kaifu²
Yutaka Hayano², Wolfgang Gaessler³ and Yukiko Kamata²

¹Subaru Telescope, 650 North A'ohoku Place, Hilo, HI 96720

²National Astronomical Observatory of Japan, 2-21-1 Osawa, Mitaka, Tokyo 181-8588, Japan

³Max-Planck institute für Astronomie, Königstuhl 17, 69117 Heidelberg, Germany

ABSTRACT

We introduce a near-infrared camera named coronagraph imager with adaptive optics (CIAO) mounted on the Subaru 8m telescope. Combined with the Subaru 36 elements adaptive optics (AO), CIAO can produce nearly diffraction limited image with ~ 0.07 arcsec FWHM at K band and high dynamic range imaging with ~ 10 mag difference at 1 arcsec separation under typical seeing conditions. We have carried out performance tests of imaging without and with coronagraph mask since its first light observation held on 2000 February. Because of limited weather conditions, the performance under best seeing conditions has not been tested yet. At a typical natural seeing condition of 0.4-0.8 arcsec, halo component of PSF using 0.2-0.8 arcsec mask can be reduced up to 70% comparing with that without mask using AO. Even after correction, residual wave front error has typically 1.2 rad^2 which corresponds to the Strehl ratio of ~ 0.3 at K band. Such wave front errors degrades the image quality; this is a common problem of coronagraph on the ground-based telescope with non high-order AO. Nevertheless we emphasize that there are various advantages on our coronagraph: the clean PSF of CIAO, reduction of readout noise, and less effect of detector memory problem. Compared with coronagraphs on smaller telescopes, the PSF shape is sharper and it brings higher detectability of sources around bright objects.

Keywords: coronagraph, high resolution camera, 8m telescope, near infrared

1. INTRODUCTION

Infrared observation techniques on the ground-based telescope have rapidly progressed and been improved since realization of adaptive optics. While previous observations have been limited as the natural seeing (eg. ~ 0.6 arcsec at Mauna Kea), currently a FWHM of ~ 0.07 arcsec at K band can be achieved with 8m class telescopes. Owing to such big progress of high angular resolution technique, high quality imaging has been requested for dynamic range as well. A technique named solar-coronagraph was originally invented by Lyot (1930)¹ and the solar corona was first detected without the total solar eclipse. In 1984, Smith & Terrile² were successful with imaging debris disk around a Vega-like star β -Pic using coronagraph optimized for non-solar objects. Now coronagraph is recognized to be a powerful instrument to detect faint objects around bright sources.

We have manufactured a near-infrared stellar coronagraph (Coronagraphic Imager with Adaptive Optics; CIAO) which allows to obtain sub-0.1 arcsec angular resolution and high dynamic range images combined with the Subaru telescope of 8.2m aperture and the 36 element adaptive optics^{3,4}. Our scientific goals are (1) detection of companion brown dwarfs and extra-solar planets around nearby stars, (2) detection of proto-planetary disks and jets around young stellar objects (YSOs), (3) imaging of circumstellar envelope around late type stars and (4) detection of circumnuclear regions around AGN and quasar host. Since its first light observation held in 2002 February, we have tested the performance of CIAO and have obtained some scientific results. In this

Further author information: (Send correspondence to K. Murakawa)

K. Murakawa: E-mail: murakawa@subaru.naoj.org, Telephone: 1 808 934 5924
Subaru Telescope, 650 North A'ohoku Place, Hilo, HI 96720, USA

paper, general information about CIAO will be summarized in section 2, results of direct imaging are reported in section 3.1, coronagraph performance is described in section 3.2 and the CIAO coronagraph advantages are argued in section 4.

2. CORONAGRAPHIC IMAGER WITH ADAPTIVE OPTICS

2.1. Configuration and Specification

Fig.1 (left) shows a configuration of CIAO, AO system and the Subaru telescope. Star light entering through telescope optics reaches adaptive optics system. Distorted wavefront of the star light is corrected by tip/tilt mirror and deformable mirror then corrected light enter into CIAO optics. Our CIAO employs Lyot's type coronagraph (Lyot 1939)¹ and all optical components are in cooled cryostat. Final image is acquired by an IR detector.

CIAO has a 1k×1k Aladdin II detector which was manufactured by Raytheon (the former Santa Barbara Research Center). The pixel size of the detector is $27\mu\text{m}\times 27\mu\text{m}$. The detector is cooled at 30 to 35K to operate in a cryostat by a closed-cycle cooler manufactured by the Sumitomo Heavy Industries, Inc. We usually use a bias level of -500 mV. The wavelength coverage is 0.9 to $5.5\mu\text{m}$. The readout noise is $25\text{ electrons s}^{-1}$ (DCS) and the dark level is less than $0.3\text{ electrons s}^{-1}$. CIAO has 3 camera lens optics. Two modes (HRM and MRM) are for imaging with 11.5 mas per pixel (FOV ~ 11.7 arcsec) and 21.7 mas per pixel (FOV ~ 22.2 arcsec), respectively. The other PIM (Pupil Imaging Mode) is for checking optical alignment between CIAO optics and the telescope optics.

A mask wheel is placed at the Cassegrain focus. The 18 optical elements are selectable. Twelve coronagraph masks (0.1 to 4.0 arcsec in diameter) are available. While the most ground-based coronagraph has 1 arcsec in diameter or larger coronagraph mask, CIAO has small masks down to 0.1 arcsec in diameter. The mask shape is a circular without any supports which can produce asymmetric artifacts on the image. The accuracy of the mask size is $2\mu\text{m}$ which corresponds to 0.004 arcsec. These masks have about 2% transmission for identify the stellar center. In fact, astrometry with an accuracy of a few tenths of the pixel scale is possible. Six kinds of stops can be selectable. These are circular Lyot stops with its diameter of 100%, 90% and 80% of the actual pupil stop. One has a cross shape with a disk at the center which is for blocking the spider pattern and telescope center hole and another has gradient transmission at the edge of the pupil. Entire optics are on the cooled optical bench and are cooled to $\sim 77\text{K}$ during operation.

Currently we have 2 filter wheels that have 10 filter positions for each. The $zJHKK_S L'M'$ broad band filters (astronomical consortium standards), 8 narrow band filters, wire grid polarizer, and ND filter are available. These configurations and measured limiting magnitudes are summarized in Table 1.

2.2. Principle of coronagraph

A schematic of Lyot's coronagraph optical configuration is shown in Fig.1 (right). The important components are coronagraph mask, which is often called occulting mask, and Lyot stop. First we consider just direct imaging before coronagraph imaging. Star image forms at the telescope focal plane and then does at the detector through collimator, pupil and camera lens of instrument. Star light forms a disk-like intensity distribution at the pupil plane and the final star image has an Airy pattern, which is so called point spread function (PSF), if the aperture has circular shape. Now we consider coronagraph configuration. Circular mask is located at the telescope focal plane and blocks the star image. A crown-like intensity distribution with its peak at the pupil edge appears. Lyot stop has 80-90% diameter of actual pupil diameter and blocks a strong intensity portion around the pupil edge. Therefore, star image drops on the mask is selectable reduced, while that which is sufficiently separated (at least twice of mask diameter) from the mask is not affected by coronagraph optics and its intensity at the final image is the almost same as that obtained by direct imaging. This phenomenon can be described using Fourier optics technique. Since smaller mask produces smoother intensity distribution at the pupil plane, smaller Lyot stop is suitable. However, coronagraph performance, spatial resolution and aperture cross-section drop in such condition. Using masks whose diameter is equal to 4 times or larger than the diameter of Airy disk gives good coronagraph performance.

Table 1. Summary of characteristics of CIAO

Detector	Aladdin II, 1024×1024 InSb array
Wavelength coverage	0.9 - 5.5 μ m
Readout noise	25 electrons (rms, DCS)
Throughput	~15% (including all optics of telescope, AO and CIAO)
Dark current	0.3 electrons s ⁻¹
Camera lens	HRM(11.5 mas pix ⁻¹ , FOV~11.7 arcsec) MRM(21.7 mas pix ⁻¹ , FOV~22.2 arcsec) PIM (for checking optical alignment)
Mask	0.1, 0.2, 0.3, 0.4 0.5, 0.6, 0.8, 1.0, 1.5, 2.0, 3.0, 4.0 arcsec in diameter circular shape with 2% transmission
Stop	3 with circular shape(100%, 90%, 80%) 1 with cross and disk at center 1 with gradient transmission
Filter	2 filter wheels <i>z</i> , <i>J</i> , <i>H</i> , <i>K</i> , <i>Ks</i> , <i>L'</i> and <i>M'</i> FeII, CH ₄ on, CH ₄ off, Hcont, H ₂ 2-1, H ₂ 1-0, Br γ , Kcont and ND
Polarimetry	half wave plate(<i>JHK</i> band, MgF ₂) wire grid polarizer(<i>J</i> to <i>M'</i> band) the Wollaston prism(<i>J</i> to <i>M'</i> band, MgF ₂)
Spectroscopy	<i>J</i> to <i>K</i> R~100-400 with 0.8-0.2 arcsec width slit
Limiting magnitude	23.4 mag(<i>J</i>), 22.1 mag(<i>H</i>), 21.9 mag(<i>K</i>), 16.5 mag(<i>L'</i>), 12.7 mag(<i>M'</i>) 1.0" diameter aperture, 5 σ , 1 hour integration time

3. RESULTS OF PERFORMANCE TEST

3.1. Direct imaging

Because of the limited weather conditions during the PV phase, our test observations were conducted under typical or mediocre seeing conditions (>0.4 arcsec). We observed a single star image without coronagraph and with AO to demonstrate the performance of image formation of the CIAO optics. The details of AO performance are described by the Subaru AO group⁴. The observation was carried out on 2002 February 21. The object is a single bright star BS2721 with $m_K=4.13$ mag. The natural seeing was ~ 0.7 arcsec in the *R* band. Elevation during this observation was $\sim 58^\circ$. Total exposure time was 0.8 sec. Fig.2 shows the *JHK* band images with FOV 4.3×4.3 arcsec². At *HK* band, central core and the first diffraction ring can be seen clearly. A X-shape artifact is due to the secondary support structure. Speckle-like patterns nearby the central core seen in *K* band image are due to the secondary support as well. Except for these patterns, PSF by CIAO is very symmetric and clean.

Fig.3 shows radial profiles of PSF with and without AO. As a comparison, a PSF resulting with the ideal wavefront and with telescope optical configuration is drawn as well. Observation without AO has been carried out in different night from that with AO. The natural seeing was 0.6 arcsec in the *R* band and there was no big difference of sky condition from that with AO. The measured FWHM and the Strehl ratio are listed in Table 2. At *H* and *K* band, nearly diffraction limited image quality was recorded. The improvement of the Strehl ratios,

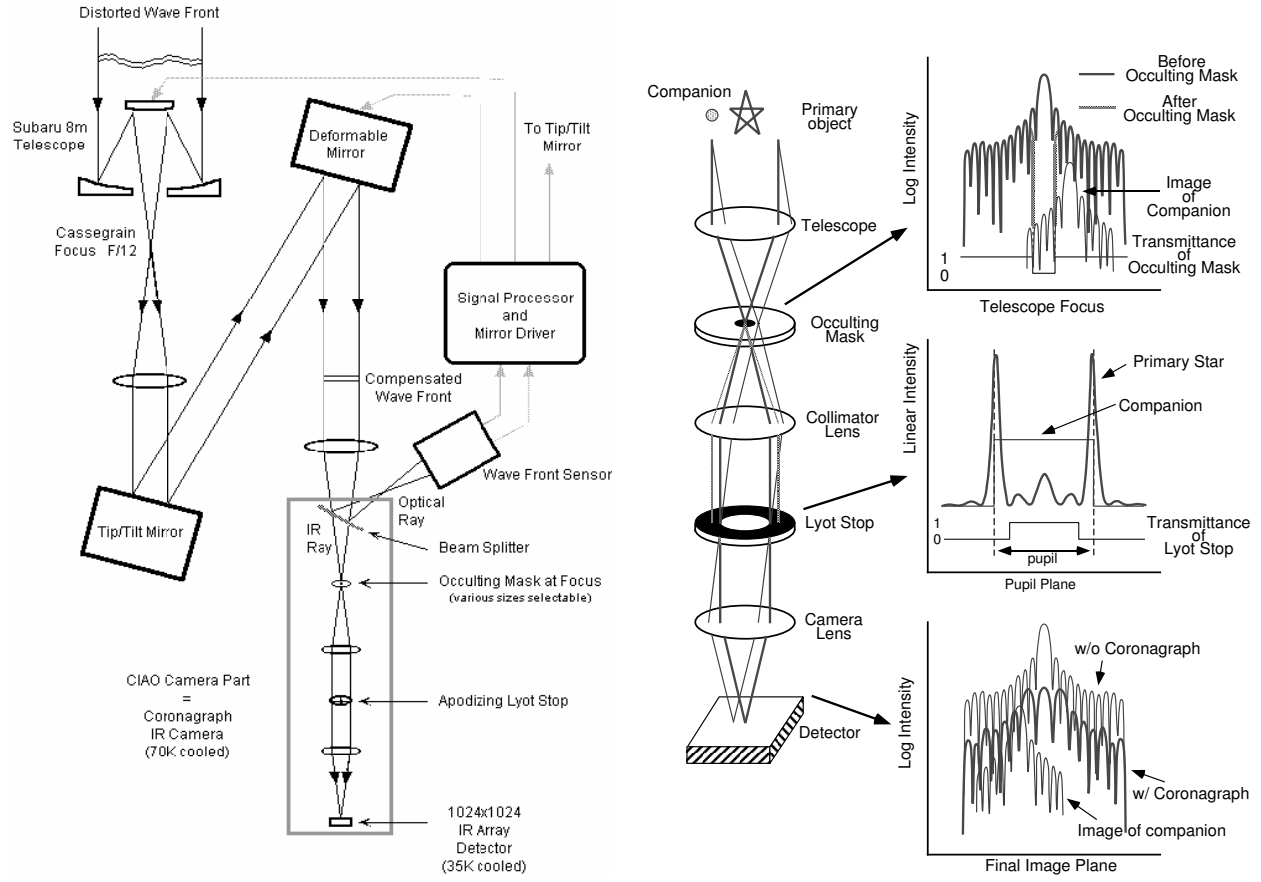


Figure 1. Configuration of CIAO, AO and the Subaru telescope (left) and principle of Lyot's coronagraph (right).

the ratio of the Strehl ratio with AO to that without AO, are 4.1, 7.4 and 9.4 at J , H and K band, respectively. While halo component without AO image exceeds more than that with AO image, core shape with AO is much sharper than that without AO.

Table 2. FWHM and the Strehl ratio of PSFs

	J band	H band	K band
Reyleigh limit	0.039"	0.051"	0.069"
FWHM w/ AO	0.15"	0.060"	0.072"
w/o AO	0.54"	0.43"	0.37"
the Strehl ratio w/ AO	0.0296	0.103	0.283
w/o AO	0.0072	0.014	0.030
improvement of the Strehl ratio	$\times 4.1$	$\times 7.4$	$\times 9.4$

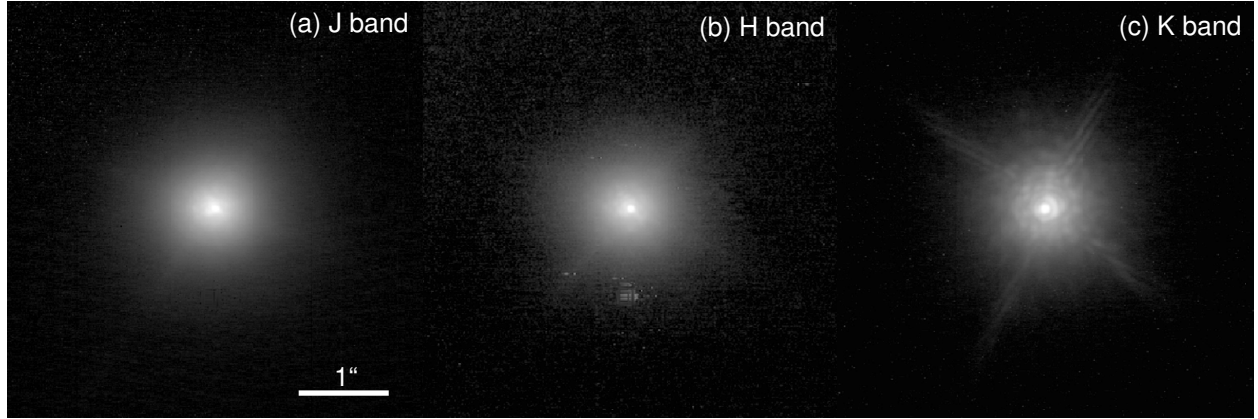


Figure 2. The *JHK* band direct imaging with AO. Scratch-like patterns below the PSF seen in *H* band image are due to residual bad pixel.

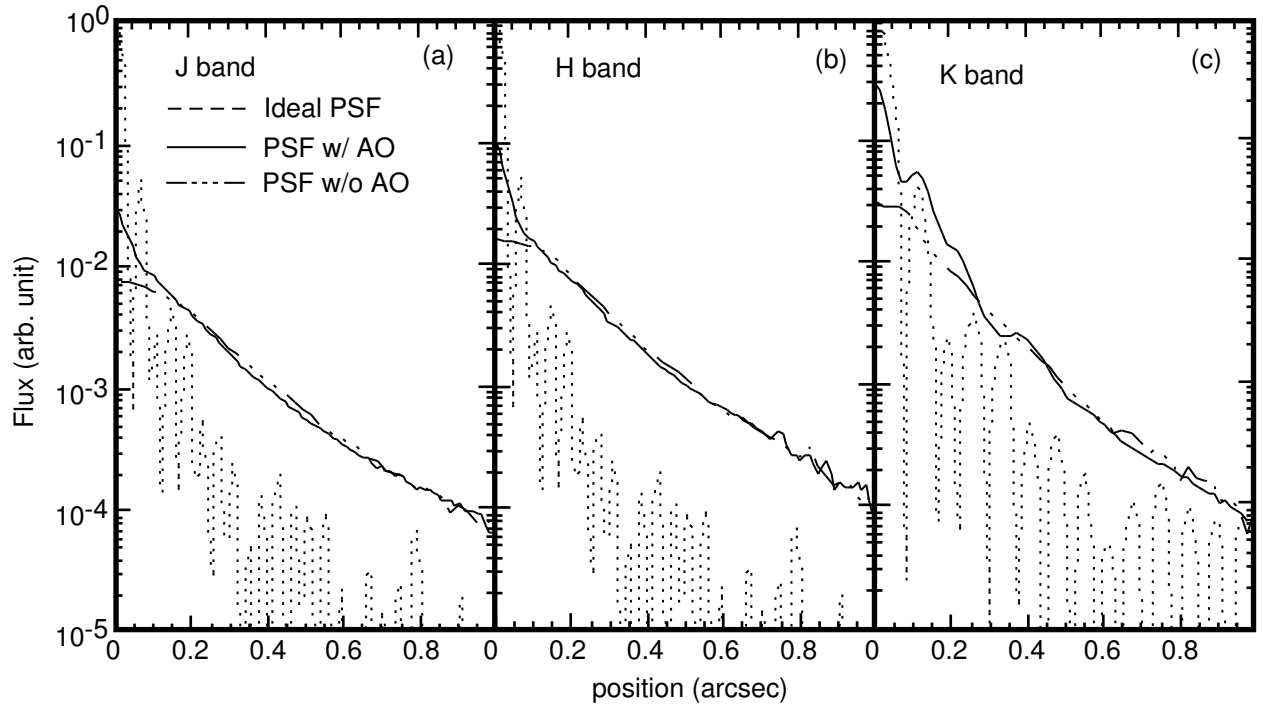


Figure 3. Radial profile of PSF. The solid curve and dashed curve denote PSF with and without AO, respectively. As a comparison, a PSF with the ideal condition is drawn with dotted curve.

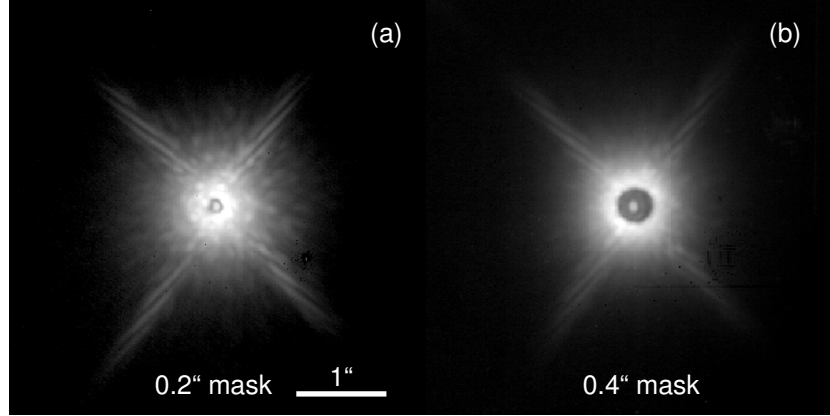


Figure 4. Coronagraph PSF using 0.2 (a) and 0.4 (b) arcsec in diameter masks. Star image can be seen through the masks and this is useful for taking alignment of object image frame by frame. Strong X-shape secondary diffraction pattern can be seen. Speckle-like patterns can be seen in particular 0.2 arcsec mask image. This is not actual speckle pattern but artifacts due to diffraction by the secondary support.

3.2. Coronagraph imaging

We also evaluate the coronagraph performance. The experiment was carried out during the same observation run as the direct imaging and the object was the same star. The total integrated exposure time was 18 sec (cf. 0.8 sec for the direct imaging). Fig.4 shows a coronagraph PSF images at K and using 0.2 and 0.4 arcsec diameter mask. It could be the first results using such small masks. The star image can be seen through these masks and that allows us to identify the stellar position and is useful for taking alignment of the image frame by frame. Fig.5 compares with radial profiles of the ideal coronagraph and PSF without coronagraph. While halo component around the star core image can be reduced $\sim 90\%$ comparing with that of direct imaging in the ideal condition, the result of actual coronagraph imaging shows limited performance and the halo component could be reduced only 20%. We show a pupil image in Fig.6 using the PIM optics. Lyot stop was removed because we are interested in just intensity distribution at the pupil plane. Although bright diffraction patterns can be seen at the edge of the spider and telescope aperture, a crown-like intensity distribution which has been explained in section 2 is not prominent in this image. This is due to residual wave front error even after AO correction. This is a common problem among any ground-based coronagraph with a non high-order AO system.

4. ADVANTAGES ON CIAO

In spite of the above limited performance, there are various advantages on our coronagraph.

First, CIAO employs small coronagraph mask down to 0.1 arcsec in diameter. The most previous ground based coronagraph as shown in Table 3 have 1 arcsec in diameter or larger mask. Using such our small mask allows us to detect objects or structures nearer the central blocked source than other instruments can do. Second, CIAO coronagraph mask has circular shape and slight transmission. CIAO's coronagraph mask is made with chromium deposition on the sapphire plates and there are no supporter for the mask. Such masks don't make any asymmetric artifacts. CIAO's mask has transmission of 2%. We have examined the effect by such transparent mask on halo component and have confirmed that no significant enhancement of halo component was seen. Such transparent coronagraph mask is useful for taking alignment of object image frame by frame and PSF reference. Third, CIAO can produce sharp and "clean" PSF. Combining with AO, FWHM reaches 0.06-0.07 arcsec and the Strehl ratio does 0.1-0.3 at HK band. That is nearly diffraction-limited images. Optical alignment can be checked using PIM optics and adjusted before observation. This is important to keep good PSF during the observation. "Clean" PSF can be produced by using a stop with 90% or 80% actual pupil diameter to avoid contamination of stray light and by using circular mask for coronagraph imaging. Fourth is a reduction of readout noise. Comparing with direct imaging, coronagraph imaging allows extending single exposure time per

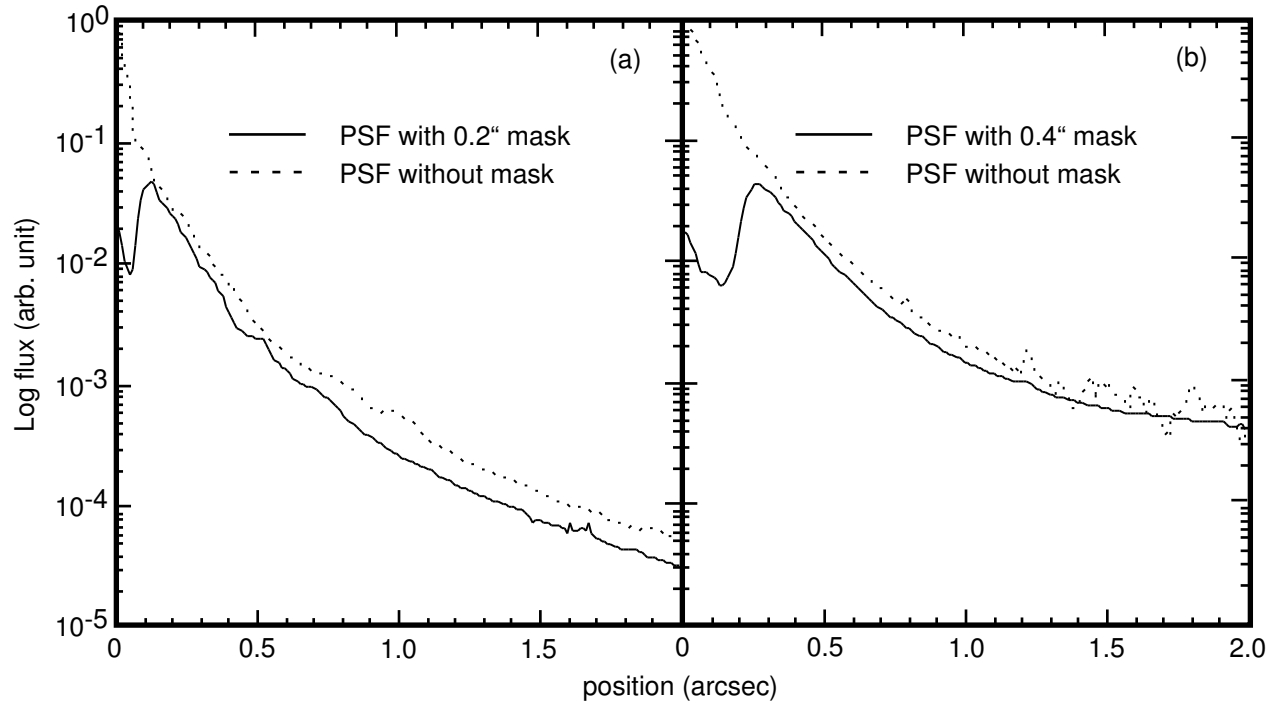


Figure 5. Comparison of radial profiles of coronagraph PSF with non-coronagraph PSF. The Fig.5a and 5b show results using 0.2 and 0.4 arcsec mask, respectively. The solid curve denotes coronagraph PSF and dotted curve denotes non-coronagraph PSF.

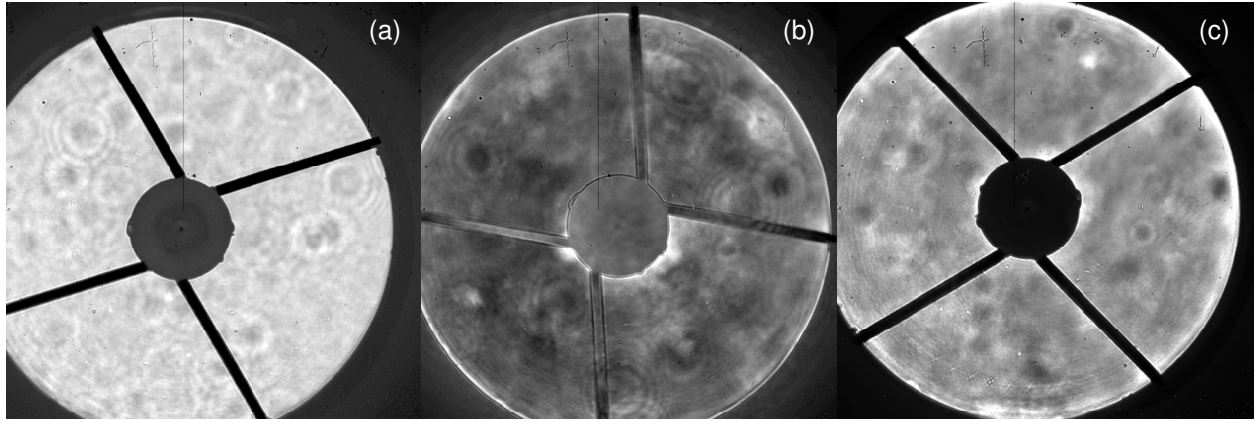


Figure 6. Pupil images of non-coronagraph mode (a) and coronagraph mode (b) and (c) obtained using PIM optics. The (b) and (c) are for 0.2 and 0.4 arcsec mask. The most flat intensity distribution is seen for non-coronagraph mode. Various circular ring-like patterns appear on images are due to actuator supporter attached backside the primary mirror. In pupil images for coronagraph mode, crown-like intensity distribution is expected by the ideal condition. However, actual images don't show clearly. Because residual wavefront error, actually 1.2 rad^2 which corresponds to the Strehl ratio of 0.3, remains even after AO correction. Such residual wavefront error makes the pupil intensity distribution flatten and results only limited performance of coronagraph.

an image acquisition avoiding saturation of detector. Coronagraph mask with 2% transmission can extend up to 50 times exposure time than direct imaging. Assuming taking same total integration time for both direct and coronagraph imaging, coronagraph imaging can reduce readout noise up to $\sim 13\%$ and longer exposure time and small number of cycles can reduce overhead time of data acquisition. Fifth is the still-high dynamic range; the companion detection limit at H band is 10 mag difference from a primary star at 6σ , 1 arcsec separation under the natural seeing of 0.6 arcsec.

Table 3. Representative optical and infrared coronagraph

Name	Telescope	AO	mask
<i>Lyot</i>	<i>Pic du Midi 20cm</i>	—	—
LPL	LC 2.5m	—	7"
JHU-AOC	Palomar 1.6m	Tip/Tilt	4-6"
UCLA	KPNO 2.1m	—	6"
Caltech	Palomar 5m	—	1"
CoCo	IRTF 3m	Tip/Tilt	3"
ADONIS	ESO 3.6m	ADONIS	0.8"
CIAO	Subaru 8.2m	36 element	$>0.1''$
NICMOS	HST 2.4m	(in space)	0.6"

ACKNOWLEDGMENTS

We would like to thank the Subaru telescope group both in Hawaii and Mitaka for their support and encouragement.

References

1. M. B. Lyot, "A study of the solar corona and prominences without eclipse", *MNRAS*, **99**, pp. 580-594, 1939
2. B. A. Smith, R. J. Terrile, "A circumstellar disk around β -Pictoris", *Science*, **226**, pp. 1421-1424, 1984
3. H. Takami, N. Takato, Y. Hayano, W. Gaessler, M. Iye, Y. Kamata, T. Kanzawa, Y. Minowa, "Performance of Subaru adaptive optics system and the scientific results", *Proc. SPIE*, **4839-03** 2002
4. M. Tamura, H. Suto, Y. Itoh, N. Ebizuka, Y. Doi, K. Murakawa, S. S. Hayashi, Y. Oasa, H. Takami, and N. Kaifu, "Coronagraph Imager with Adaptive Optics (CIAO): Description and First Results", *Proc. SPIE*, **4008**, p. 1153, 2000